

Aerial Scene Parsing

From Tile-level Scene Classification to Pixel-level Semantic Labeling

Gui-Song Xia

School of Computer Science, Wuhan University
Institute of Artificial Intelligence, Wuhan University
State Key Lab. LIESMARS, Wuhan University

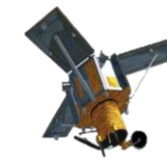


Advanced RS Technology



CAPTAIN
COMPUTATIONAL AND PHOTOGRAHMETRIC VISION

RS technology has significantly improved the Earth observation ability.

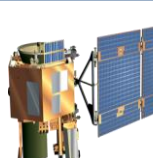
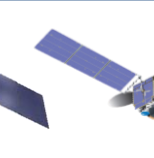
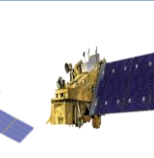
							
LandSat-1	LandSat-4	Spot-1	IKONOS	QuickBird	WorldView-1	GeoEye-1	WorldView-3
1972	1975	1978	1982	1984	1986	1990	1993
LandSat-1 78m 18d	LandSat-2 78m 18d	LandSat-3 78m 18d	LandSat-4 30m 16d	LandSat-5 30m 16d	Spot-1 10m 26d	Spot-2 10m 26d	Spot-3 10m 26d
1998	1999	2001					
Spot-4 10m 26d	IKONOS	QuickBird 0.61m 1-6d					
2002	2003	2007	2008	2009	2011	2012	2014
Spot-5 2.5m 26d	OrbView-3 1m 3d	WorldView-1 0.5m 1.7d	GeoEye-1 0.41m 2-3d	WorldView-2 0.5m 1.1d	Pleiades-1A 0.5m 1d	Spot-6 1.5m 1d	WorldView-3 0.31m <1d
2016	2021						
WorldView-4 0.31m <1d	Legion 0.29m 15t/d						
							SCOUT 0.29m 24t/d

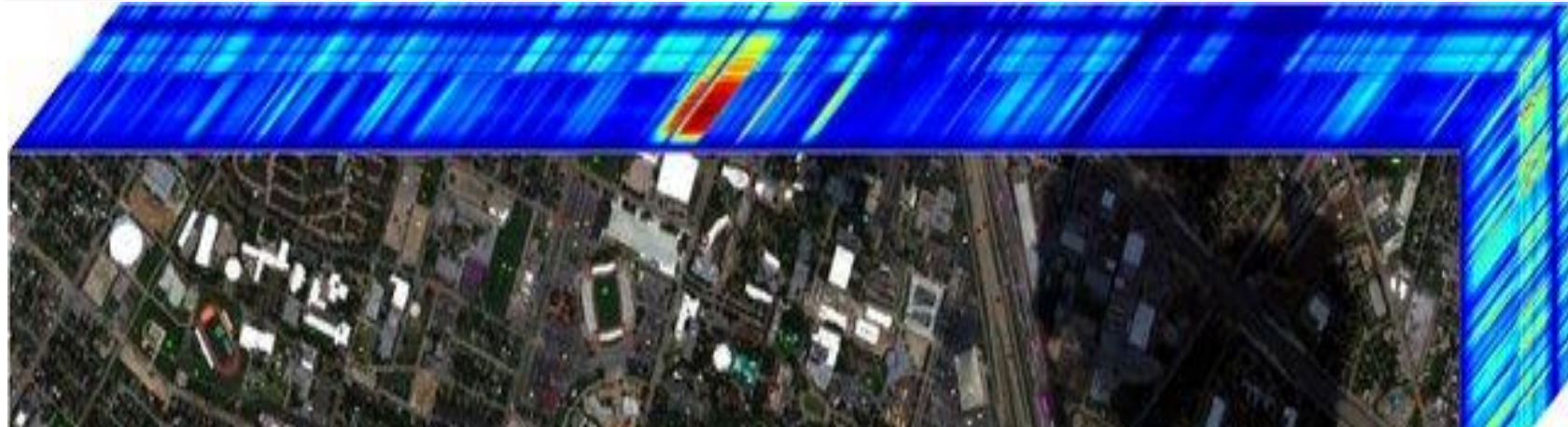


The characterization of features on the earth surface.

Advanced RS Technology

RS technology has significantly improved the Earth observation ability.

										
LandSat-1	EOS AM-1	MightySat II	EO-1	ISS DESIS	GF-5	TEMPO	JPSS-2			
1972	1986	1999	2000	2000	2002	2008	2018	2018	2018	
LandSat-1 8 0.475-12.6	NOAA-10 20 0.669-14.5	EOS AM-1 36 0.62-14.385	MightySat2.1 145 0.45-1.05	EO-1 220 0.4-25	ADEOS-2 115 0.45-0.95	IMS-1 64 0.4-0.95	HJ-1A 115 0.45-0.95	ISS 235 0.4-1.0	HysIS 316 0.4-2.4	GF5 330 0.4-2.5
2019	2020	2021	2022	2022	2022	2024	2024	2024	>	
PRISMA 240 0.4-2.5	HyperScout2 45 0.4-14.0	GISAT-1 150 0.9-2.5	EnMAP 232 0.42-2.45	TEMPO 666 0.29-0.74	JPSS-2 1305 3.9-15.3	FLEX 300 0.5-0.78	MTG-S1 1720 4.6-14.3	METOP-SG A1 3936 0.270-2.385	METOP-SG A1 16921 3.62-15.5	



The characterization of features on the earth surface.

Applications of RS Images

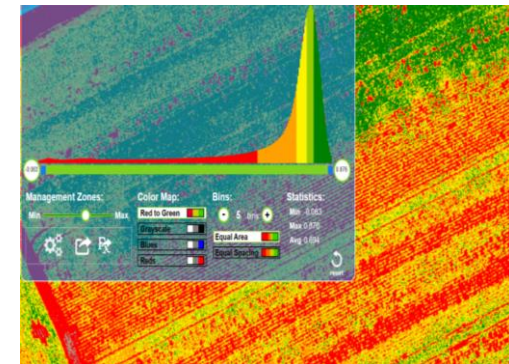
Interpretation of RS images plays important roles in many real-world applications



Information investigation



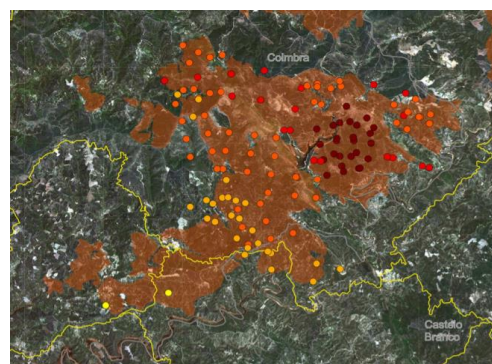
Smart city



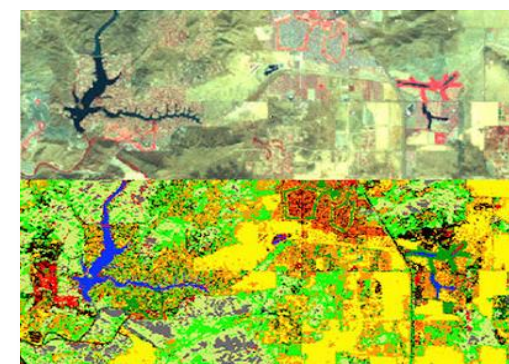
Agriculture production



Environ. monitoring



Disaster assessment



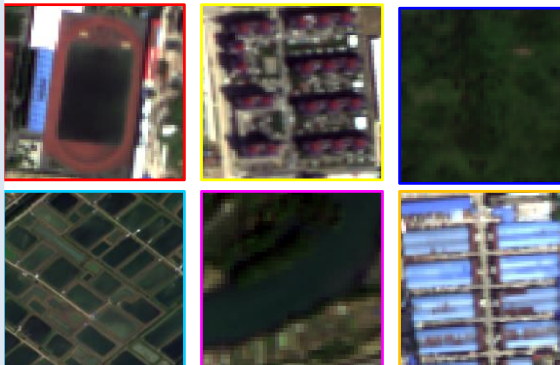
Land cover mapping

Examples

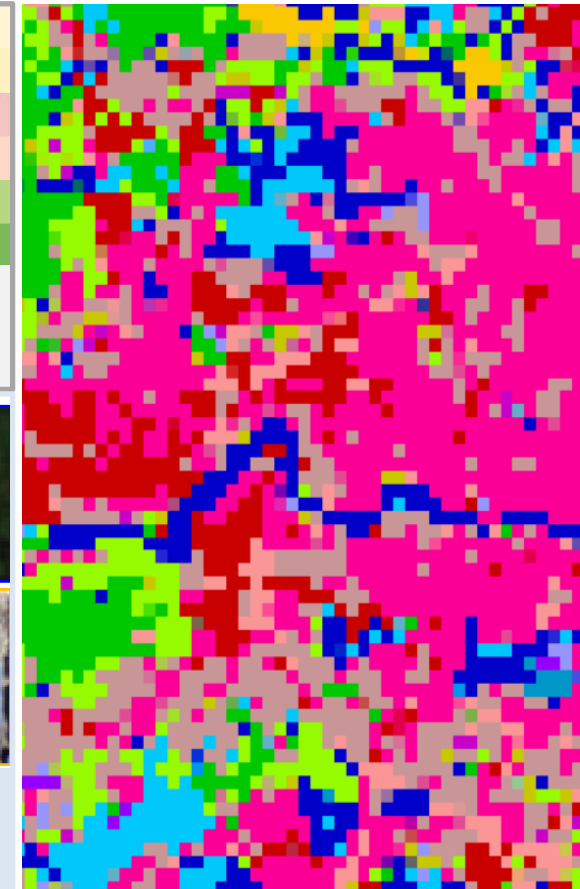
Pixel-based classification for low resolution aerial image interpretation



Individual pixels featured by distinct content of large area



Each pixel presents a scene of specific semantic category

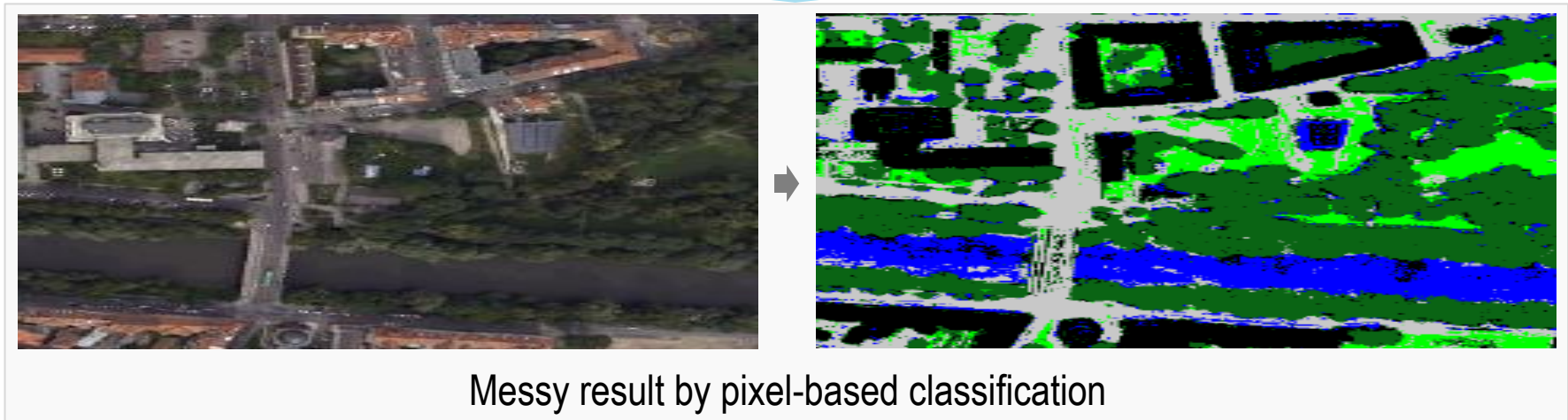
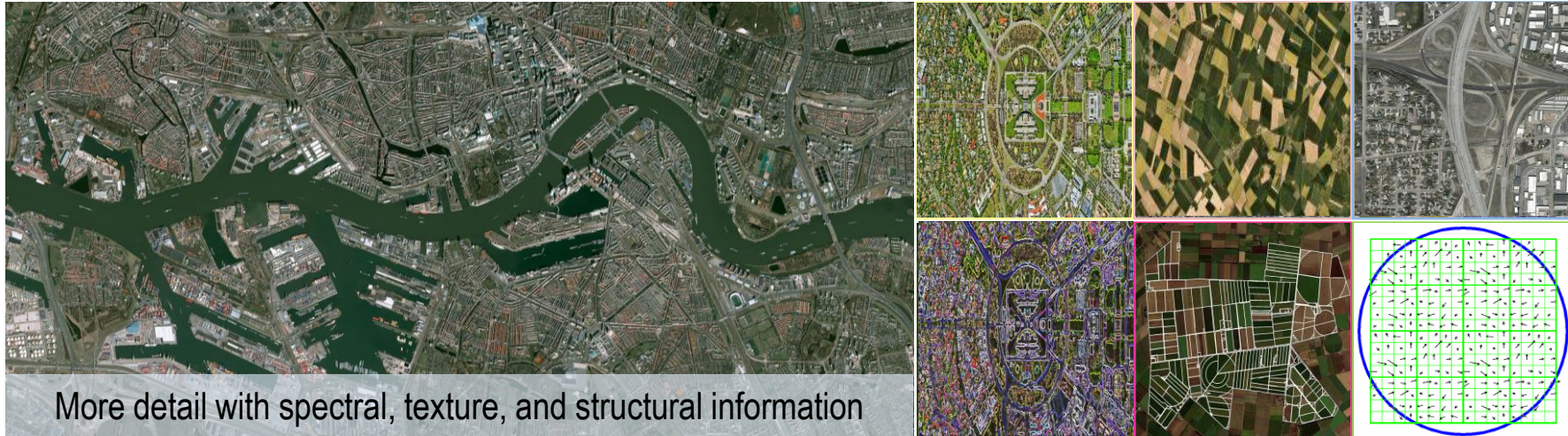


Low resolution image

Pixel-based classification

Examples

Pixel-based representation for high resolution aerial image classification

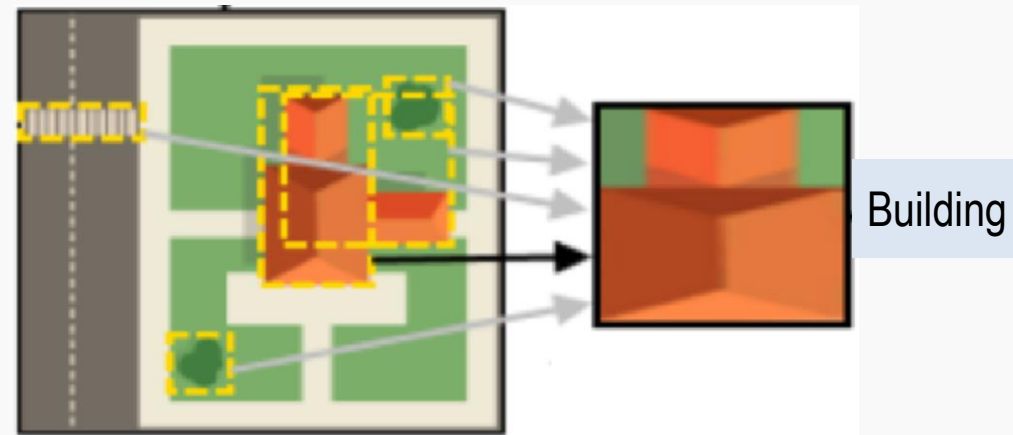


Examples

Pixels in a block belong to the same semantic class in high resolution image



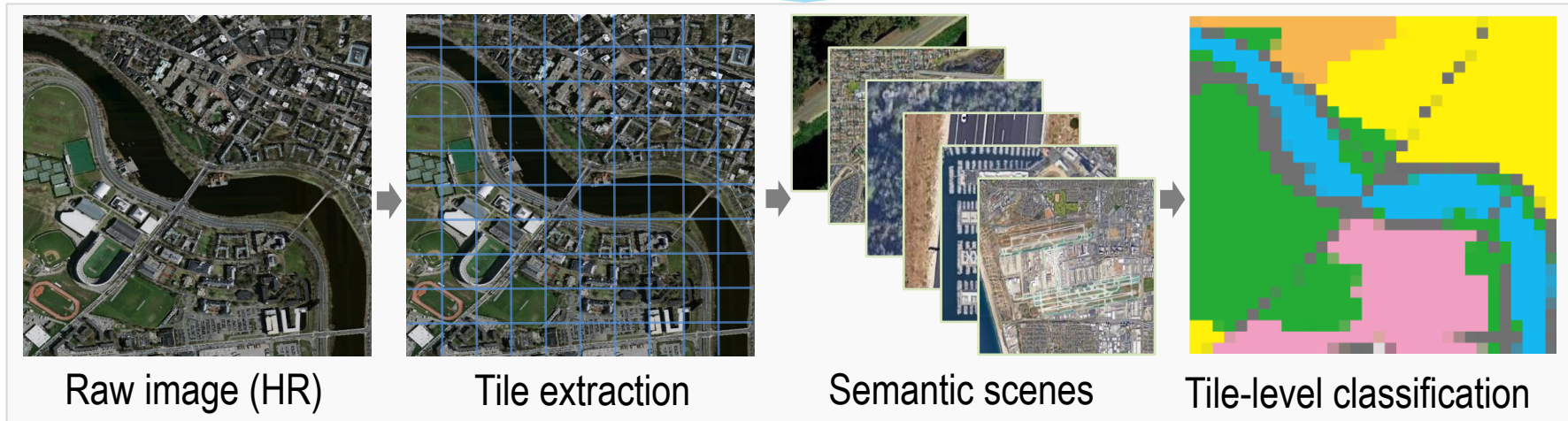
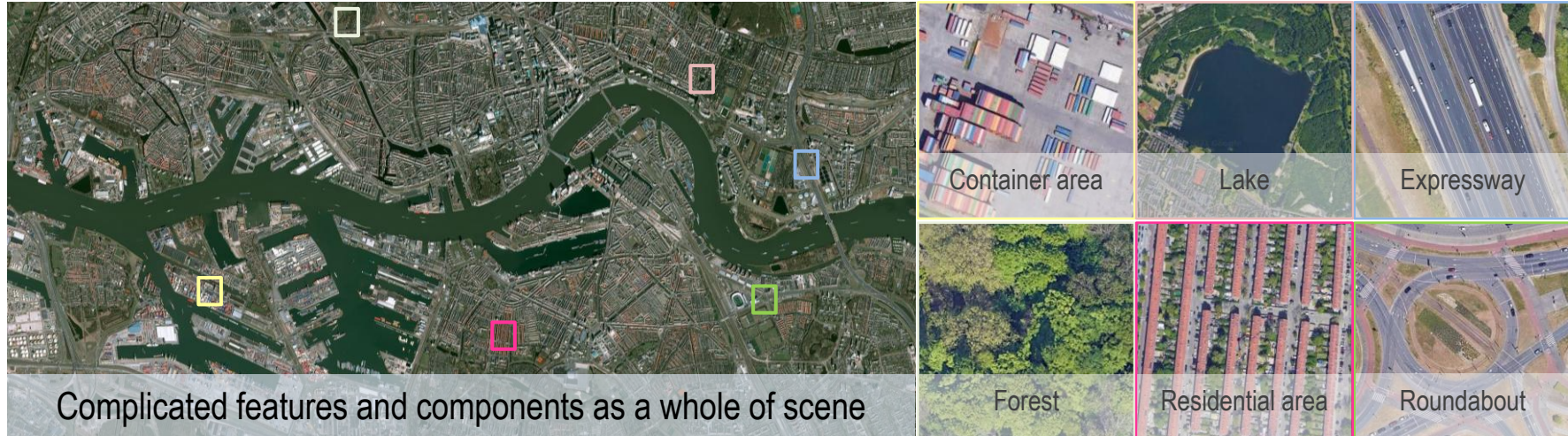
OBIA homogeneous segments
lacking semantic description



Relation modeling for different segments is required for semantic scene recognition

Examples

Tile-based representation for high resolution aerial image classification



Road Map



CAPTAIN
COMPUTATIONAL AND PHOTOGRAHMETRIC VISION

Interpretation prototypes develop with the improvement of aerial image quality



Low resolution

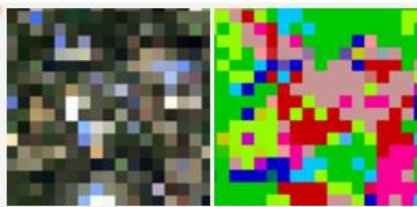
High resolution

Per-pixel classification

Object-based classification

Tile-level classification

Pixel-level semantic parsing



Spectral and textural attributes of pixels are mainly employed for semantic classification

Spectral and textural description: @R.M. Haralick et al-TSMC1973. @M.J. Swain et al-IJCV1991. @B.S. Manjunath et al-TPAMI1996. @T. Ojala et al-TPAMI2002. @G.-S. Xia et al-IJCV2010.

Statistical analysis: @L. Bruzzone et al-TGRS1999. @C.H. Chen et al-PR2008. @J. Li et al-TGRS2010/2011.

@G. Camps-Valls et al-SPM2013. @J. Zhao et al-TIP2016.

Learning classifiers: @T. Kavzoglu et al-IJRS2003. @H. Lee et al-NIPS2007. @G. Mountrakis et al-ISPRS2011.

@M. Belgui et al-ISPRS2016. @D. Lu et al-IJRS2007.

Subpixel classification: @ P. M. Atkinson-IGIS1997.

@F. Wang-TGRS1999. @B. Somers et al-RSE2011.



More rich spectral, textural, structural, and contextual detail for homogenous segmentation

OBIA paradigm: @T. Blaschke et al-GIS2001/ISPRS2014.

Spectral-spatial segment: @H.D. Cheng et al-PR2001. @B. Kaur et al-ICECT2011. @X. Han et al-ISPRS2018.

@Y. Tang et al-ISPRS2020. @R. Shang et al-ISPRS2021.

Morphological methods: @X. Zhang et al-ISPRS2014. @J. Liu et al-ISPRS2015. @J. Yang et al-RSE2017. @T. Su-ISPRS2019. @T. Su et al-ISPRS2020. Review @M. D. Hossain et al-ISPRS2019.

Deep learning segment: @E. Maggio et al-TGRS2016. OCNN @C. Zhan et al-RSE2018. @V. S. Martins et al-ISPRS2020. Review @S. Li et al-TGRS2019.



Complicated visual features and components as a whole for scene image recognition



Hierarchical scene parsing: @S.C. Zhu et al-IJCV2010.

Low-/mid-level features: @Y. Yang et al-ACMGIS2010. @S. Chen et al-TGRS2015. @Y. Zhong et al-TGRS2015. @G. Cheng et al-PIEEE2017. @G.S. Xia et al-TGRS2017.

Deep learning schemes: Transfer learning @F. Hu et al-RS2015. Feature fusion @E. Li et al-TGRS2017. Metric learning @G. Cheng et al-TGRS2018. Attention mechanism @Q. Wang et al-TGRS2019. Architecture search @A. Ma et al-ISPRS2021. Datasets @Y. Long et al-JSTARS2021.



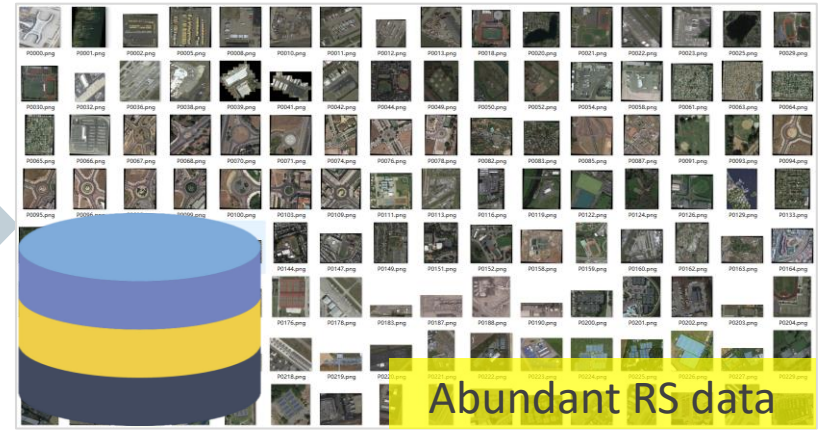
Bridging tile-level scene classification toward pixel-level semantic parsing for high resolution aerial images

High-quality Classification



CAPTAIN
COMPUTATIONAL AND PHOTOMETRIC VISION

Current situation: Increasing demand for high-quality semantic classification



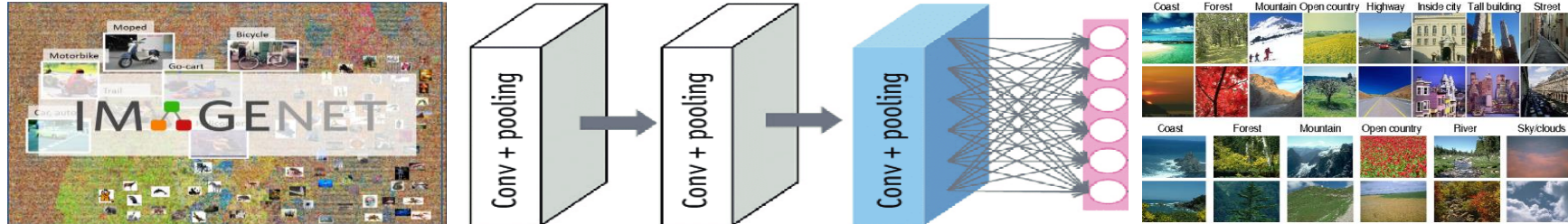
Coarse result by tile-level classification and high computational cost for pixel-wise classification

Model Adaption

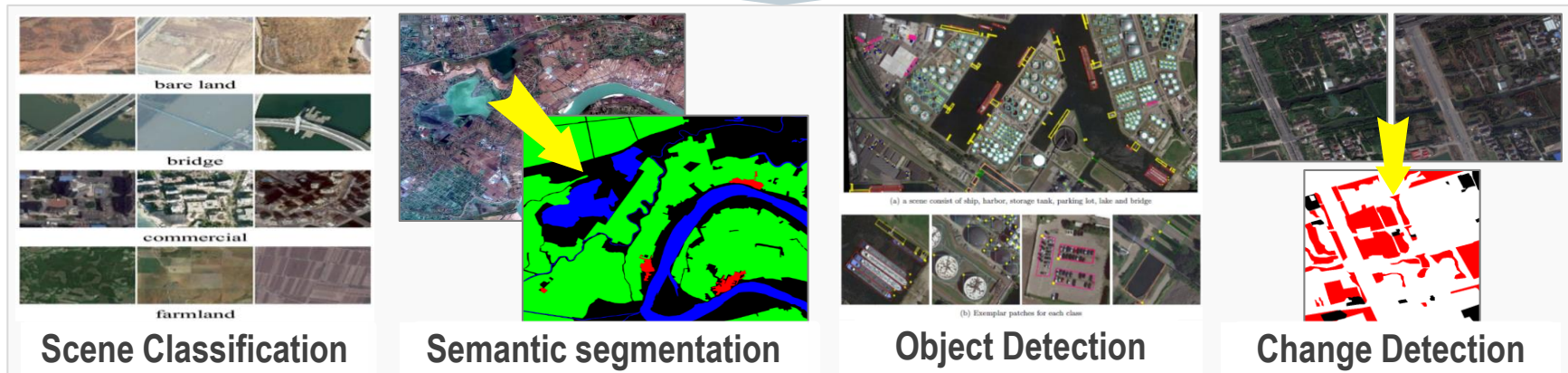
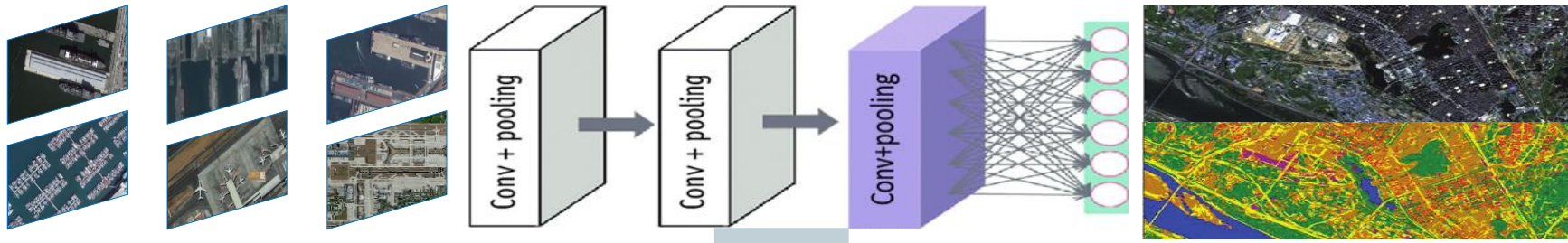


CAPTAIN
COMPUTATIONAL AND PHOTOGRAHMETRIC VISION

Model optimization: parameters from natural images transferred for RS images

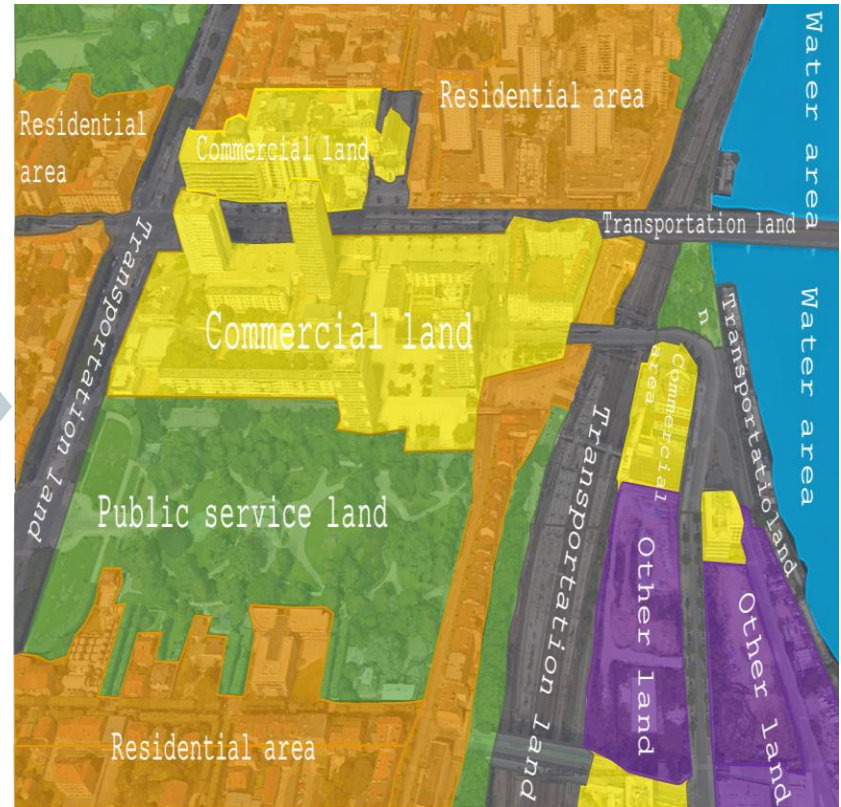


Model transfer



Interpretation of RS Images

Image classification: transfer raw imagery data into semantic information



■ Bridging tile-level classification toward pixel-level parsing

- Emphasis on **tile-level interpretation** with high-level semantics while neglecting their **homogeneous components in pixel level**.
- **Pixels** are no longer isolated units, of which semantics are highly related to their **contextual information** in high-resolution RS images.

■ Weak generalization ability of interpretation methods

- **Potential of data-driven interpretation methods** remains to be further liberated and evaluated by large-scale available datasets.
- **Insufficiency in learning and utilizing domain knowledge** from relevant interpretation data and tasks.

Outline

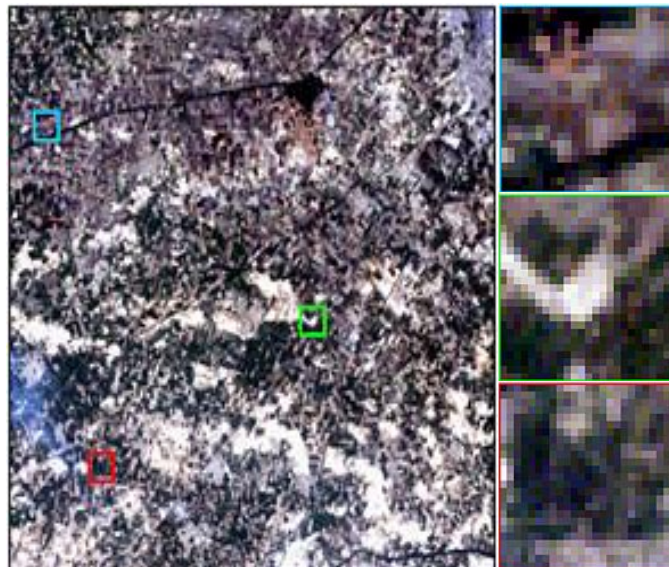


- Background
- Revisiting Aerial Scene Recognition
- Introduction to Million-AID
- Aerial Scene Classification: A New Benchmark
- Knowledge Transfer: From Tile-level to Pixel-level
- Conclusions

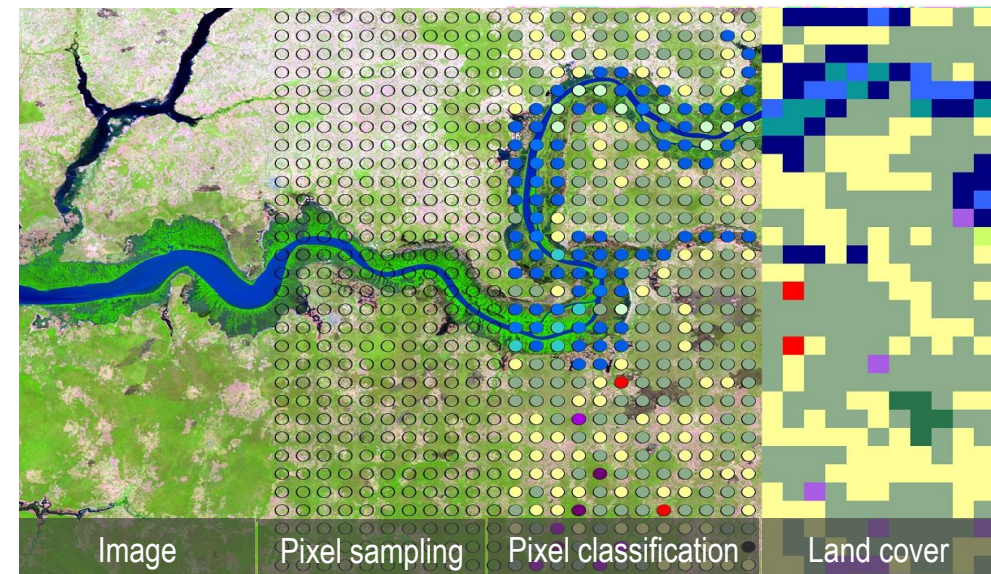
Per-pixel Classification

■ Aerial images with low resolution

- Sizes of objects are smaller than the image resolution
- Spectral and texture attributes are mainly employed
- Pixel sampling and statistical analysis with content attributes



Low resolution image



Pixel-wise image classification

Object-based Analysis

■ Objects as Basic Units

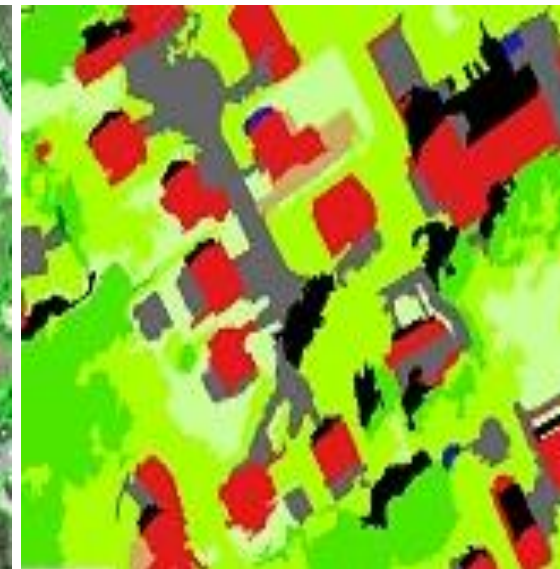
- Ground objects composed of pixels with improved resolution
- Homogeneous segmentation by spectral, texture, and structural attributes
- lack semantic description, object relation modeling, scale challenge



Image with rich detail



Homogenous segments

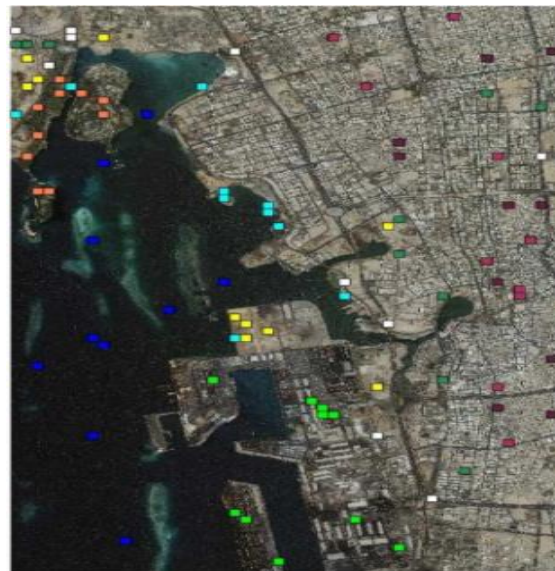


Object classification

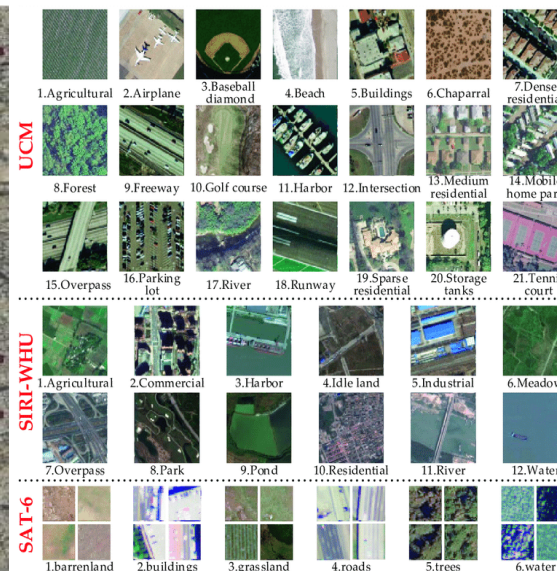
Tile-level classification

Scene recognition within local area

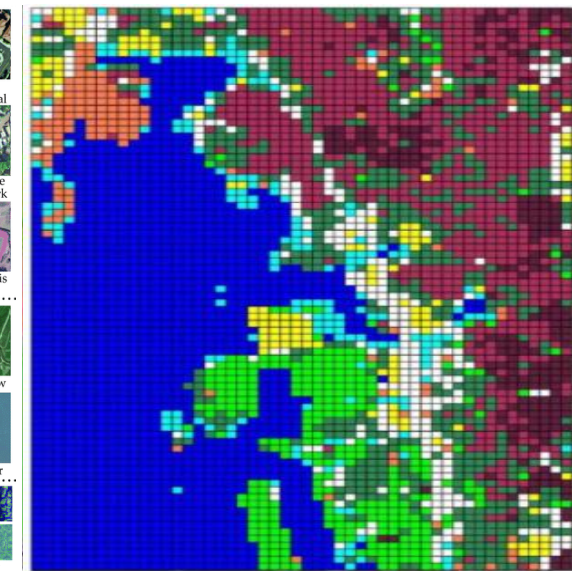
- Complicated features and content as a whole with high-level knowledge
- Scene representation from handcrafted to deep learning features
- Coarse interpretation result, accuracy saturation of existing datasets



Real-world complex content



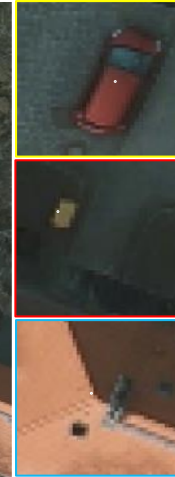
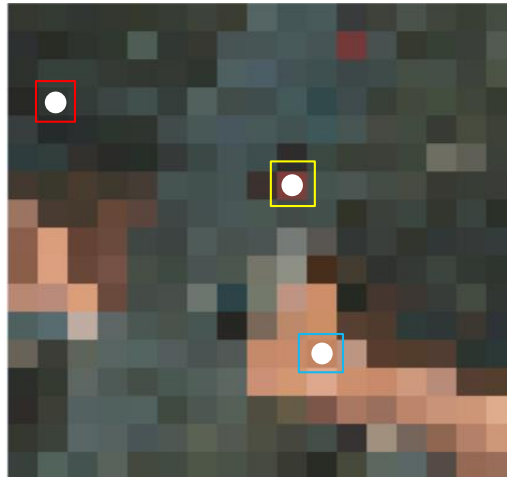
Limited classes and scale



Course classification result

Analysis

Pixels are highly related to neighborhoods in high resolution aerial images



Low resolution:
Isolated pixels as basic semantic units

High resolution:
Pixels must be considered with contextual information

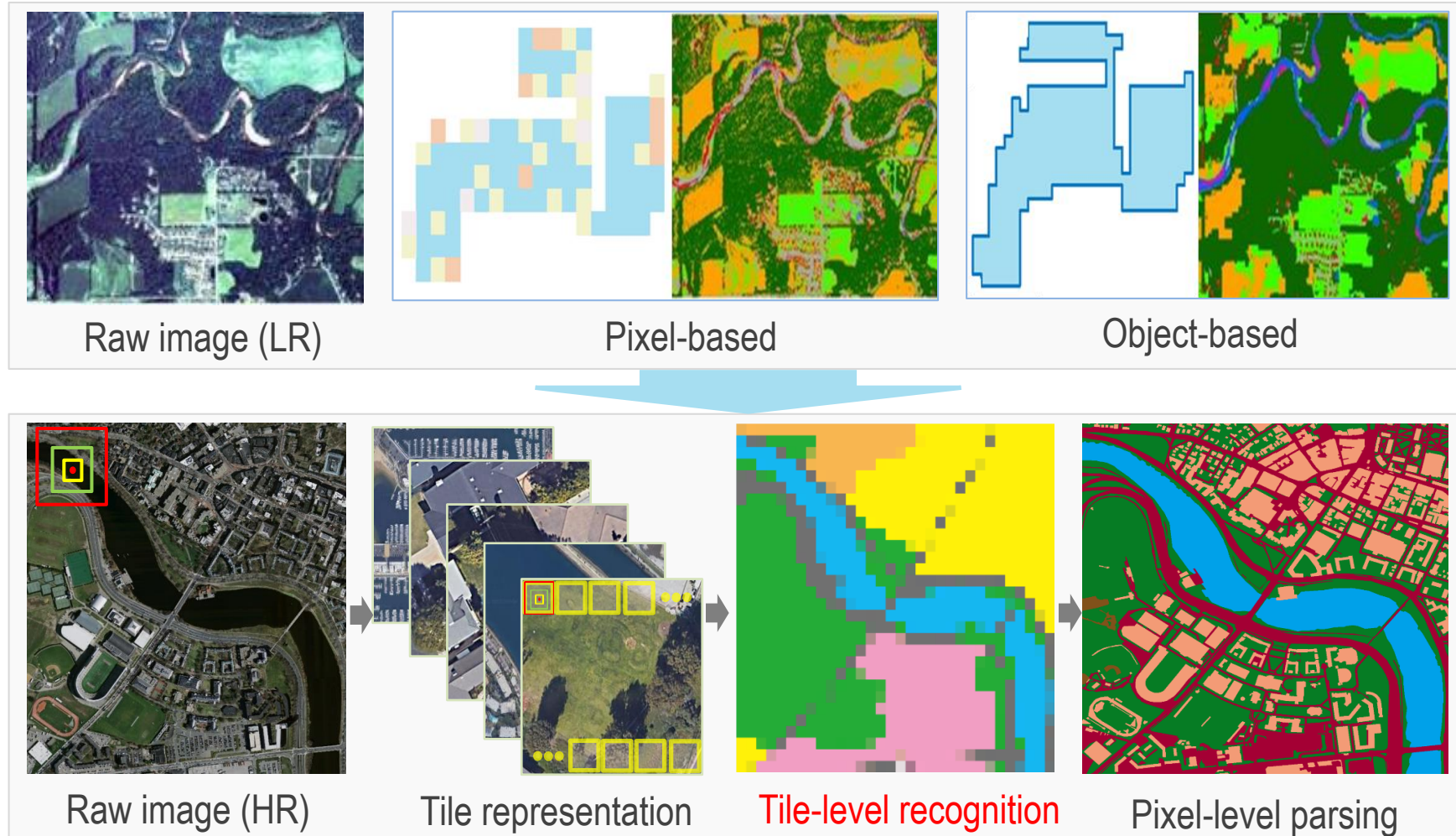
Enlarged areas of homogeneity



More rich detail with
Noisy information

Analysis

Tile-level representation for high resolution aerial image classification



Outline



- Background
- Revisiting Aerial Scene Recognition
- **Introduction to Million-AID**
- Aerial Scene Classification: A New Benchmark
- Knowledge Transfer: From Tile-level to Pixel-level
- Conclusions

Tile-level Datasets

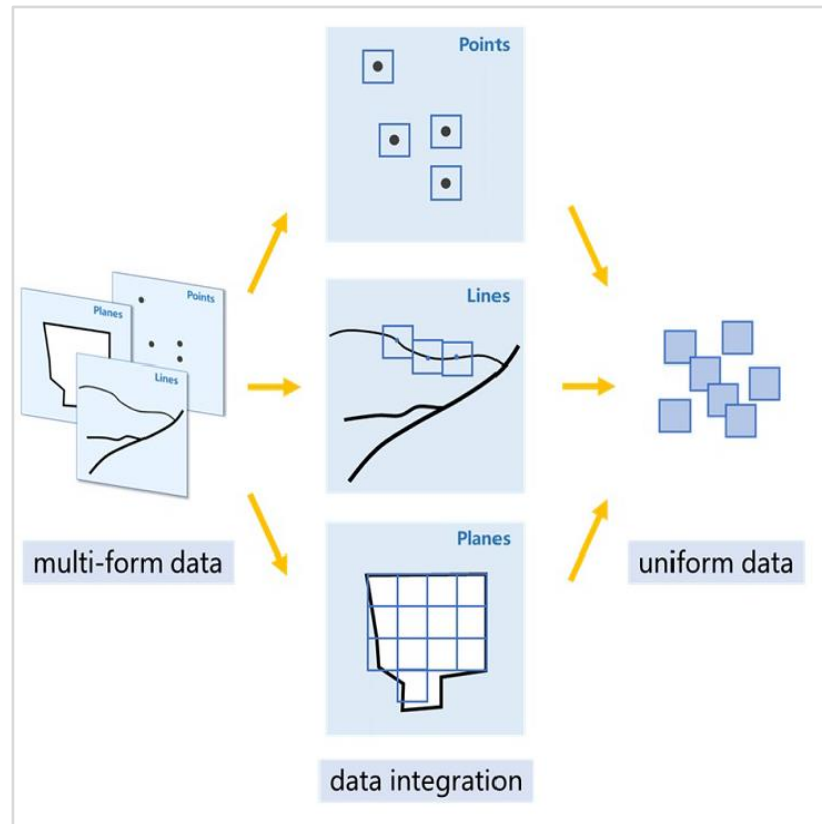
■ Aerial scene datasets

- **Small scale and poor diversity:** small number of categories and instances
- **Accuracy saturation:** lack standard evaluation benchmarks

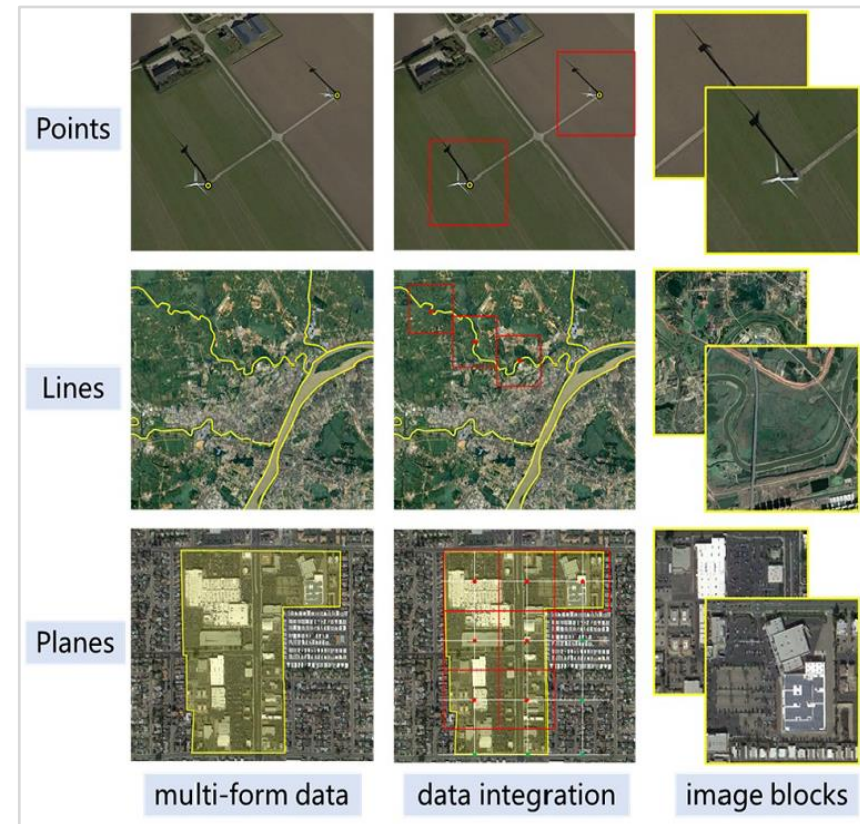
Dataset	#Cat.	#Images per cat.	#Images	Resolution (m)	Image size	GL/IT/SP	Year
UC-Merced	21	100	2,100	0.3	256×256	XXX	2010
WHU-RS19	19	50 to 61	1,013	up to 0.5	600×600	XXX	2012
RSSCN7	7	400	2,800	--	400×400	XXX	2015
SAT-4	4	89,963 to 178,034	500,000	1 to 6	28×28	XXX	2015
SAT-6	6	10,262 to 150,400	405,000	1 to 6	28×28	XXX	2015
BCS	2	1,438	2,876	--	600×600	XXX	2015
RSC11	11	~100	1,232	~0.2	512×512	XXX	2016
SIRI-WHU	12	200	2,400	2	200×200	XXX	2016
NWPU-RESISC45	45	700	31,500	0.2 to 30	256×256	XXX	2016
AID	30	220 to 420	10,000	0.5 to 8	600×600	XXX	2017
RSI-CB128	45	173 to 1,550	36,000	0.3 to 3	128×128	XXX	2017
RSI-CB256	35	198 to 1,331	24,000	0.3 to 3	256×256	XXX	2017
Planet-UAS	17	--	40,408	3 to 5	256×256	✓✓✓	2017
RSD46-WHU	46	500 to 3,000	117,000	0.5 to 2	256×256	XXX	2017
MASATI	7	304 to 1,789	7,389	--	512×512	XXX	2018
EuroSAT	10	2,000 to 3,000	27,000	10	64×64	✓✓✓	2018
PatternNet	38	800	30,400	0.06 to 4.7	256×256	XXX	2018
fMoW	62	--	132,716	0.5	74×58 to 16184×16288	✓✓✓	2018
WiDS Datathon 2019	2	--	20,000	3	256×256	XXX	2019
Optimal-31	31	60	1,860	--	256×256	XXX	2019
BigEarthNet	43	328 to 217,119	590,326	10,20,60	20×20,60×60,120×120	✓✓✓	2019
CLRS	25	600	15,000	0.26 to 8.85	256×256	XXX	2020
MLRSN	46	1,500 to 3,000	109,161	0.1 to 10	256×256	XXX	2020

Dataset Construction

- Semi-automatic scene image collection: integration of public geographical features



Geographical point, line, and plane features



Scene image interpretation

Semantic Categories

■ Hierarchical category organization with land use standard

- First-level:
8 categories
- Second-level:
28 categories
- Third-level:
37 categories



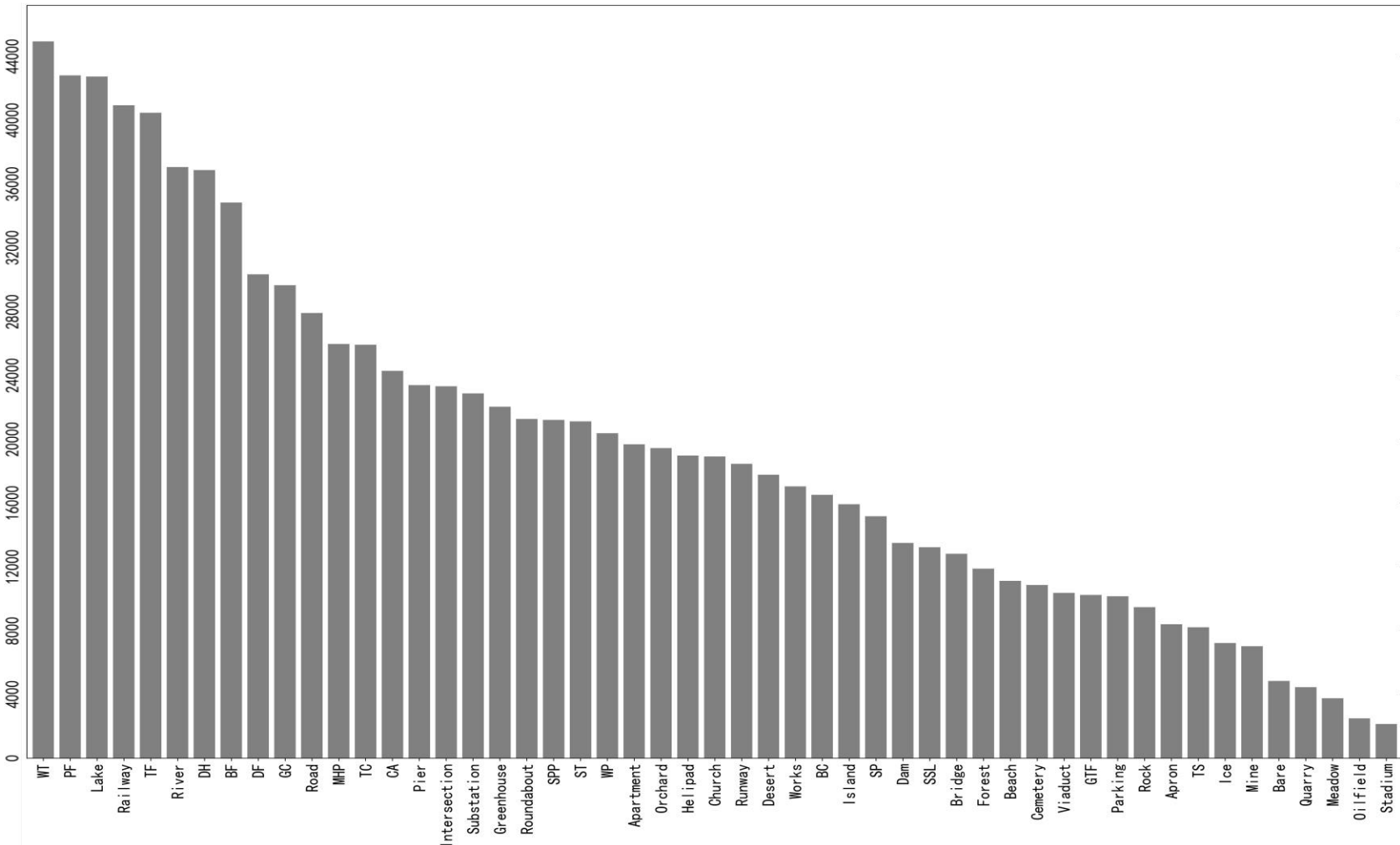
Multi-class classification:
51 fine-gained classes

Multi-label classification:
73 hierarchical classes

Agricultural land								Commercial land			
Arable land				Grassland		Woodland		Commercial area			
Dry land	Greenhouse	Paddy field	Terraced field	Meadow	Forest	Orchard					
Public service land											
Basketball court	Tennis court	Baseball field	Ground track field	Golf course	Stadium	Cemetery	Church	Religious land			
Industrial land											
Wastewater tank	Storage tank	Oil field	Works	Solar	Wind turbine	Substation	Mine	Mining area			
Transportation land											
Airport area			Highway area								
Apron	Heliport	Runway	Roundabout	Parking lot	Intersection	Bridge	Viaduct	Road			
Transportation land					Unutilized land						
Railway area		Port area			Rock land	Bare land	Ice land	Island	Desert		
Train station	Railway	Pier							Sparse shrub		
Residential land					Water area						
Detached house	Apartment	Mobile home park	Beach	Lake	River			Dam			

Dataset Scale

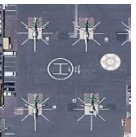
- Over 1M instances with unbalanced distribution: 2k to 45k samples in each category



Dataset Diversity

- Over 1M instances with unbalanced distribution: 2k to 45k samples in each category

Scene diversity



Apron

Baseball field

Similarity



Bridge

Viaduct

Scale variation



Storage tank

Wind turbine

Complex.

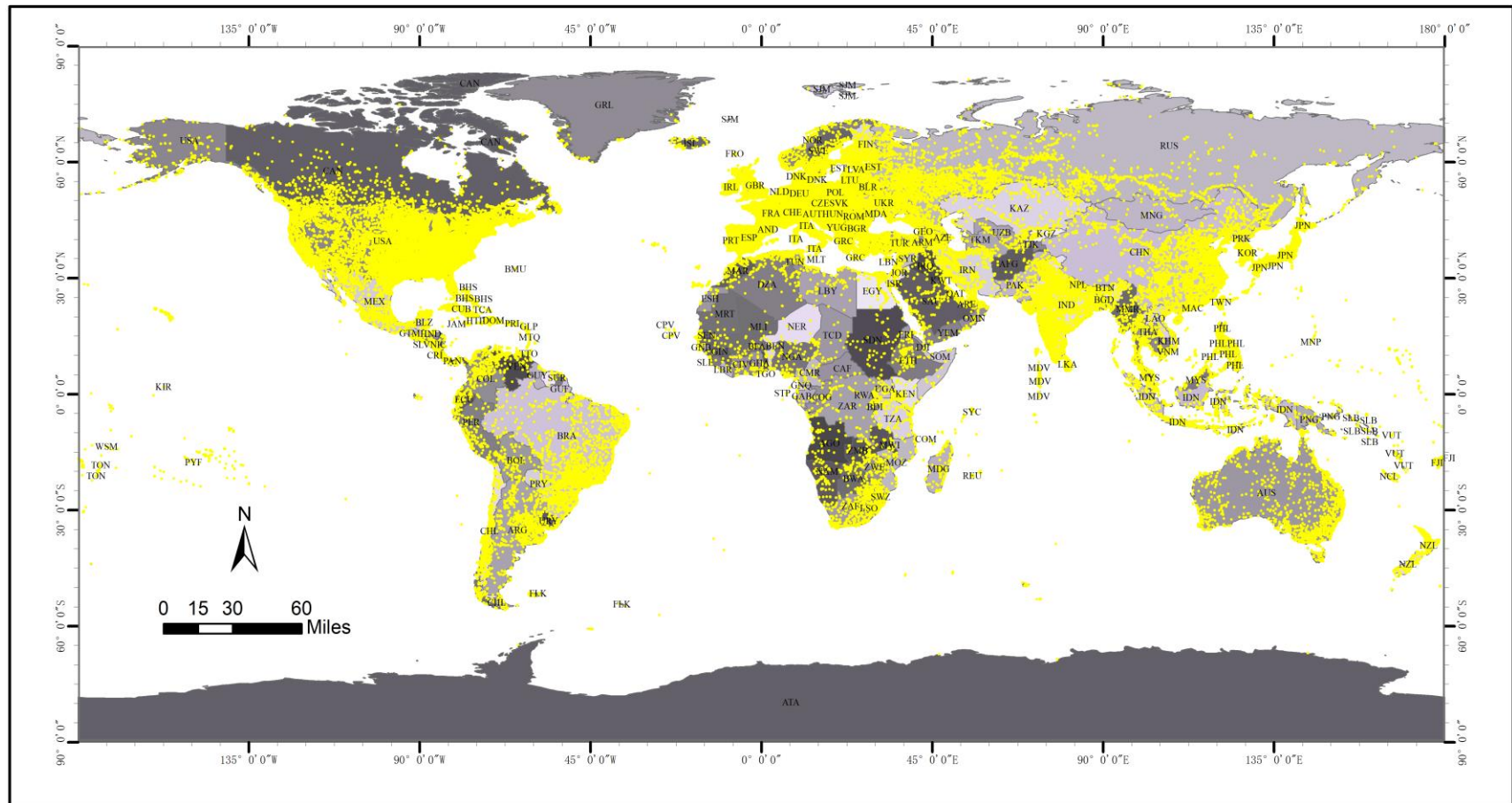


Substation

Wastewater plant

Geographical Distribution

- Scenes around the world: intensively distributed within human inhabited areas



Outline



- Background
- Revisiting Aerial Scene Recognition
- Introduction to Million-AID
- **Aerial Scene Classification: A New Benchmark**
- Knowledge Transfer: From Tile-level to Pixel-level
- Conclusions

■ Unified implementation of CNN library

Model	#Layers	#Param.	Acc@1 (%)	Year
AlexNet	8	60M	56.52	2012
VGG16	16	138M	73.36	2014
GoogleNet	22	6.8M	69.78	2014
ResNet101	101	44M	77.37	2015
DenseNet121	121	8M	74.43	2017
DenseNet169	169	14M	75.60	2017

■ Benchmarking configurations

- **Multi-class scene classification:** 51 fine-gained scene categories
- **Multi-label scene classification:** 73 semantic categories

■ Evaluation metrics

- **Multi-class scene classification:** overall accuracy (OA), average accuracy (AA), Kappa coefficient, mean of intersection-over-union (mIoU)
- **Multi-label scene classification:** per-class precision (CP), recall (CR), F1 (CF) and overall precision (OP), recall (OR), F1 (OF)

Results

■ Results of Multi-class scene classification

Performance of Single-label Scene Classification with different CNN models

Metric	AlexNet	VGG16	GoogleNet	ResNet101	DenseNet121	DenseNet169
OA	67.53	77.47	77.37	77.36	79.04	78.99
AA	63.18	74.58	74.86	74.58	76.67	76.67
Kappa	66.61	76.84	76.73	76.73	78.46	78.46

■ Results on different datasets with our framework

OA Comparison Among Different Datasets

Dataset	AlexNet	VGG16	GoogleNet
AID [16]	86.86	86.59	83.44
AID*	88.79	93.72	92.24
NWPU-RESISC45 [166]	85.16	90.36	86.02
NWPU-RESISC45*	87.19	92.76	91.71
Million-AID	67.53	77.47	77.37

* Results using our implemented CNN framework,

Confusion Matrix



CAPTAIN

COMPUTATIONAL AND PHOTOGRAMMETRIC VISION

■ Shallow network: AlexNet

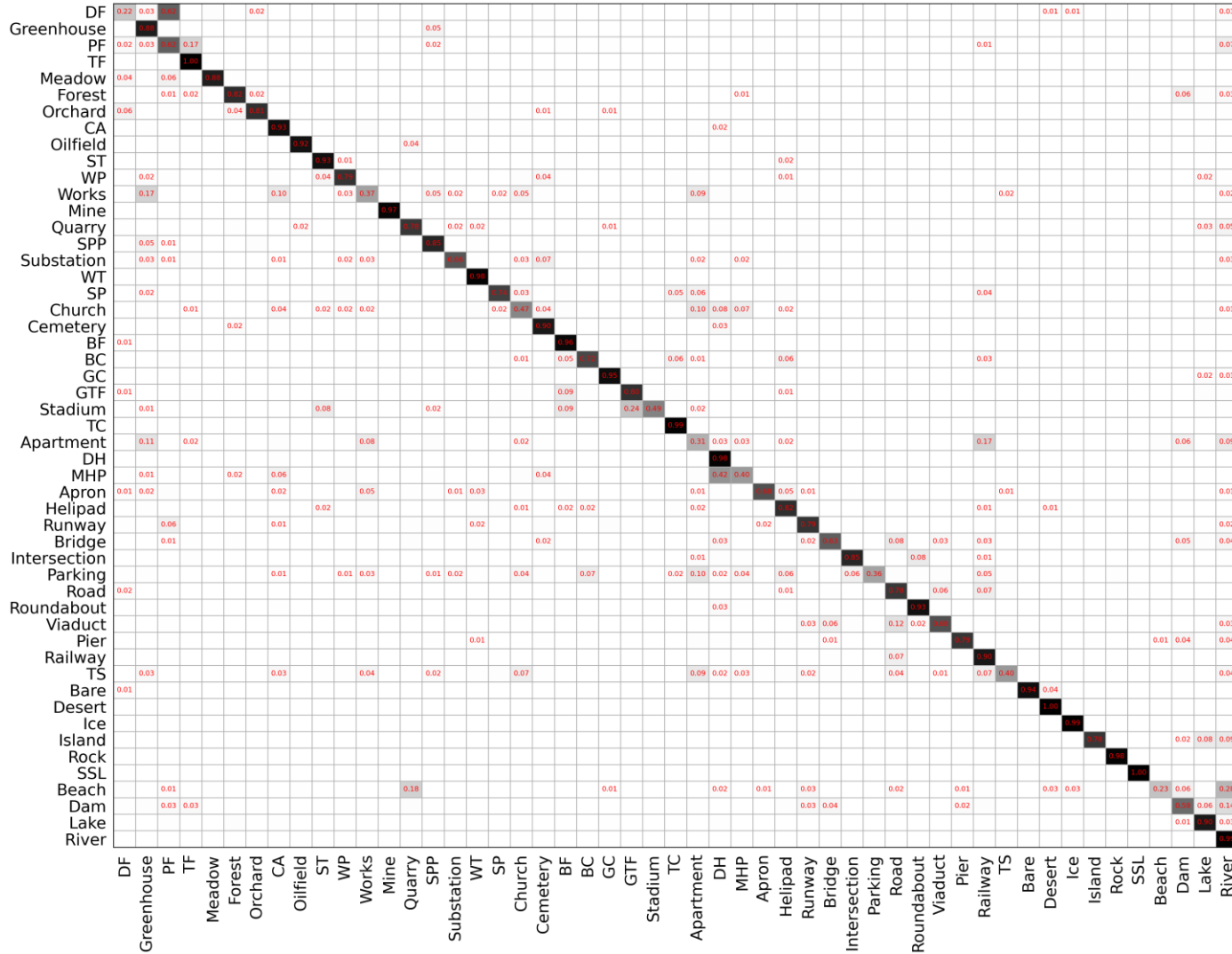
Confusion Matrix



CAPTAIN

COMPUTATIONAL AND PHOTOGRAMMETRIC VISION

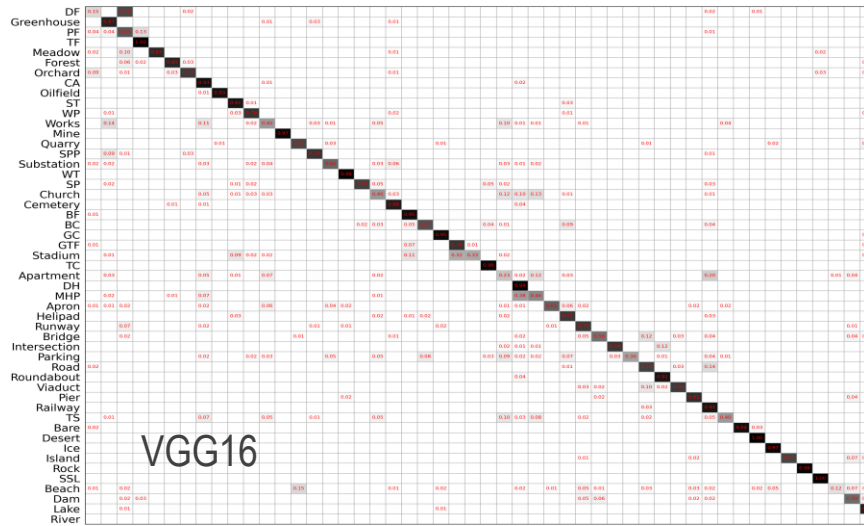
■ Deep network: DenseNet121



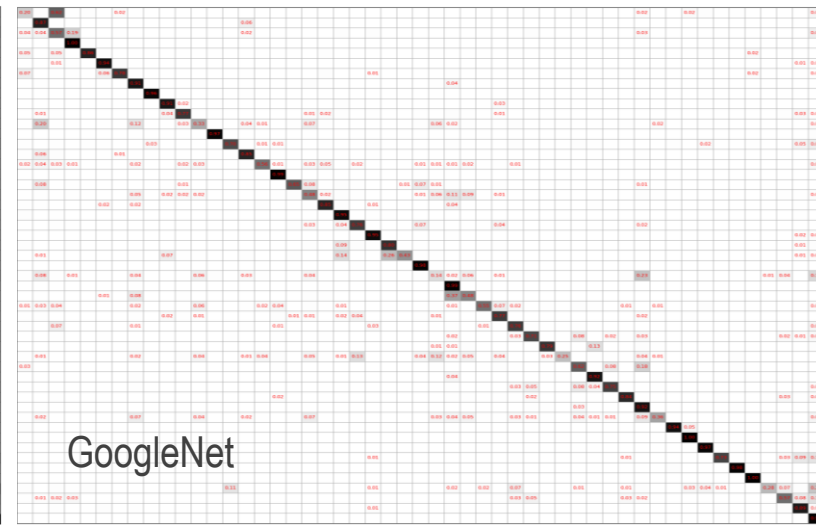
Confusion Matrix



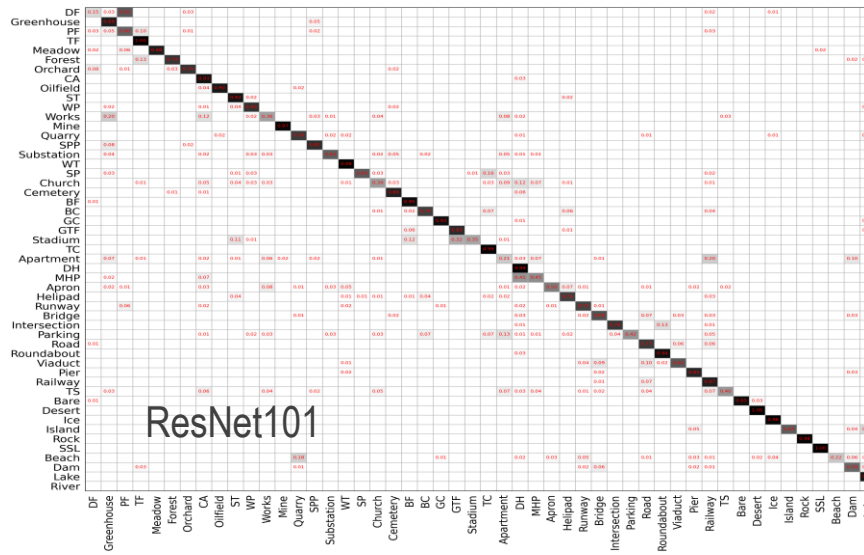
■ More results



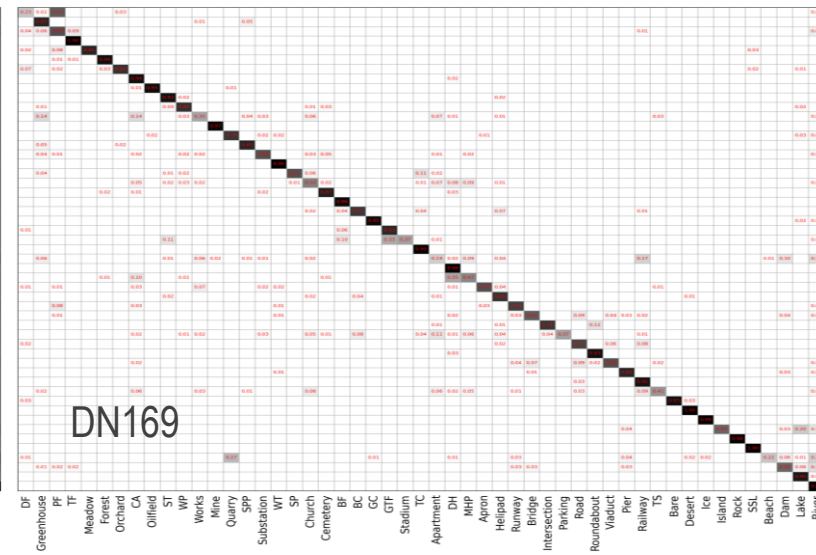
VGG16



GoogleNet



ResNet101



DN169

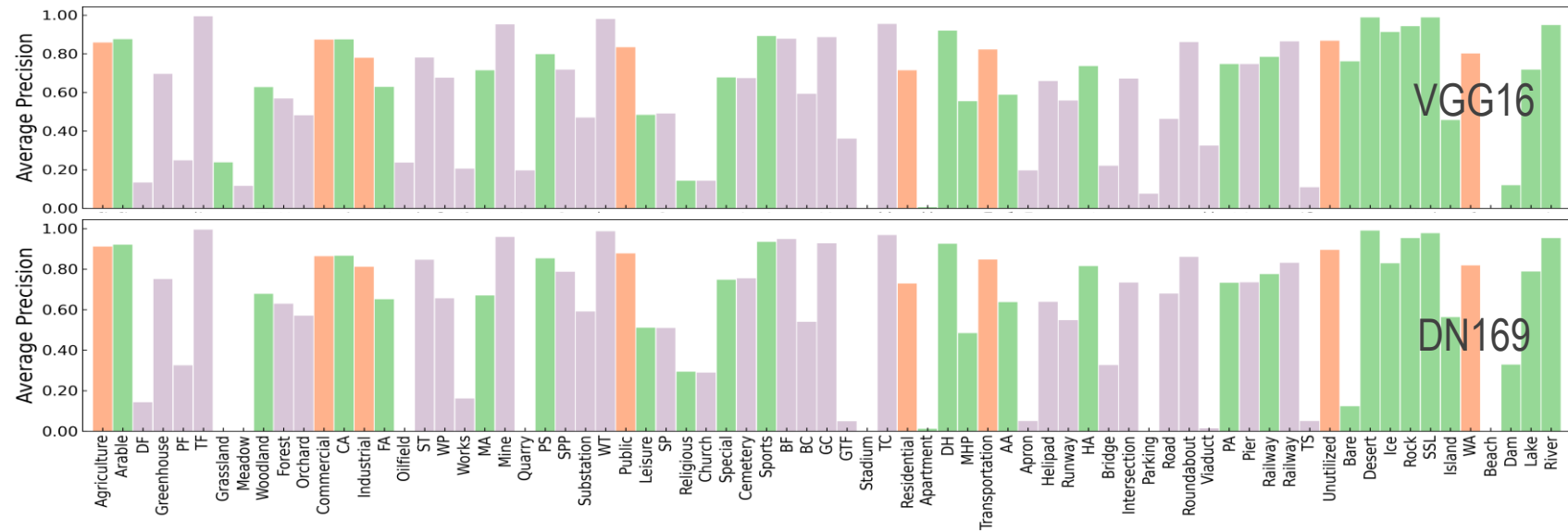
Results

■ Results of Multi-label scene classification

Performance of Multi-label Scene Classification with different CNN models

Model	$\tau = 0.5$							$\tau = 0.75$						
	CP	CR	CF1	OP	OR	OF1	mAP	CP	CR	CF1	OP	OR	OF1	mAP
AlexNet	71.45	48.19	57.56	76.19	62.84	68.87	44.20	78.89	38.51	51.76	85.65	53.03	65.50	36.52
VGG16	82.26	62.20	70.84	86.98	75.31	80.72	60.05	84.61	54.29	66.14	91.70	69.37	78.99	53.10
GoogleNet	51.79	33.99	41.04	88.50	59.47	71.14	32.96	50.99	23.76	32.42	94.90	47.02	62.89	23.36
ResNet101	79.38	59.67	68.13	88.74	77.31	82.63	57.78	76.83	51.56	61.71	93.05	70.93	80.50	50.43
DenseNet121	79.09	56.21	65.71	89.74	75.10	81.77	54.63	76.36	47.75	58.76	94.20	67.72	78.79	46.86
DenseNet169	78.54	61.92	69.24	88.50	78.55	83.23	59.75	78.52	55.10	64.76	92.66	73.10	81.72	53.66

■ Challenging hierarchical multi-label classification: “catastrophic forgetting” problem



Outline

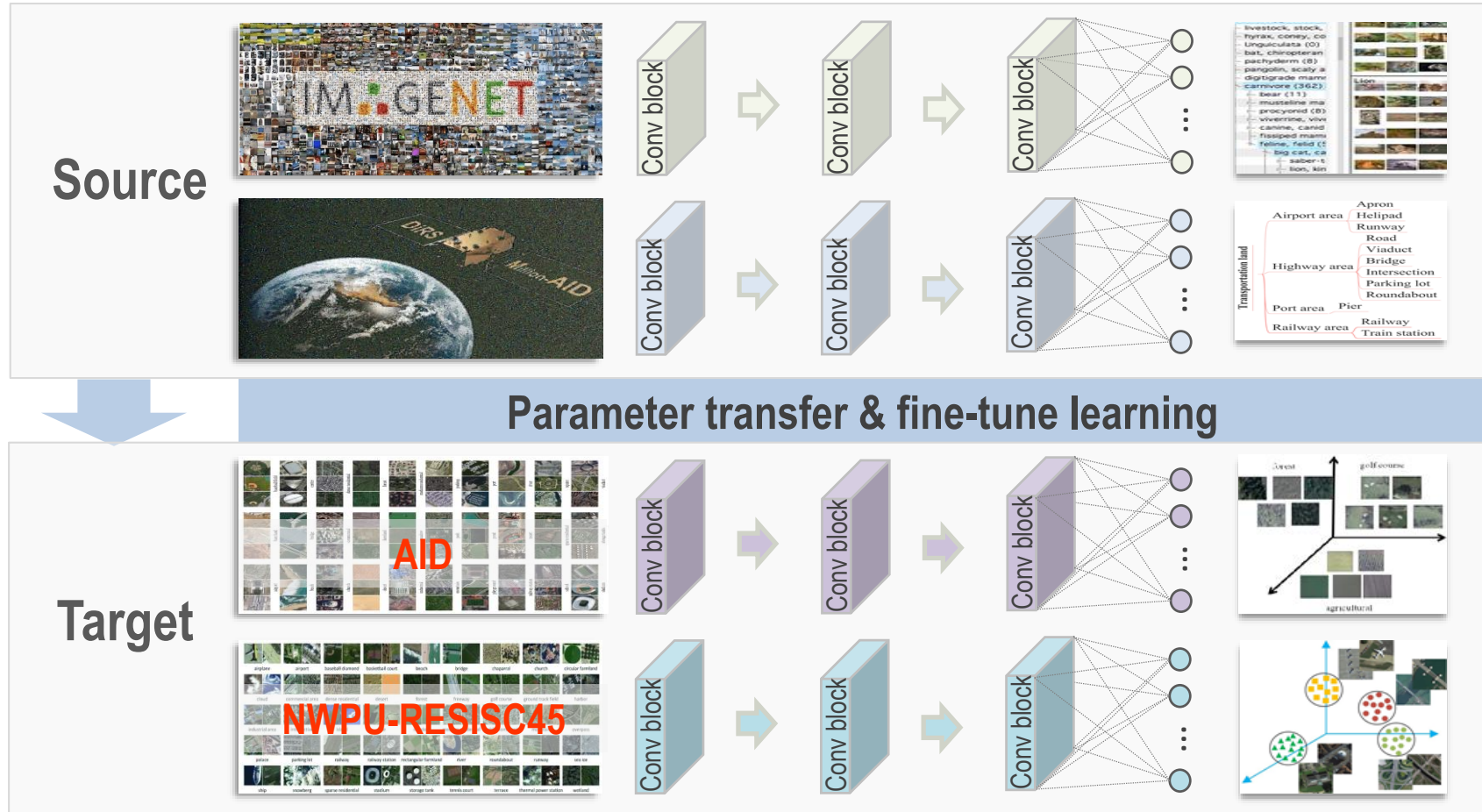


- Background
- Revisiting Aerial Scene Recognition
- Introduction to Million-AID
- Aerial Scene Classification: A New Benchmark
- Knowledge Transfer: From Tile-level to Pixel-level
- Conclusions

Scene Recognition



■ Transfer Knowledge from ImageNet and Million-AID for scene recognition



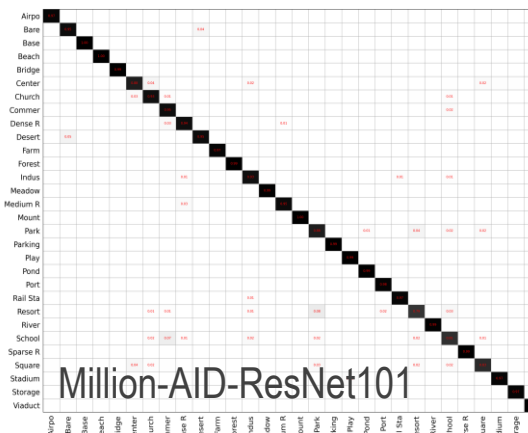
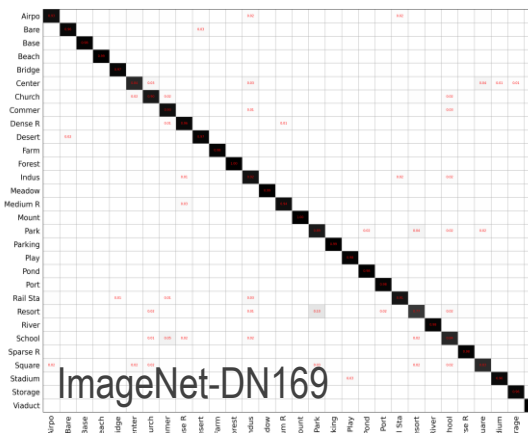
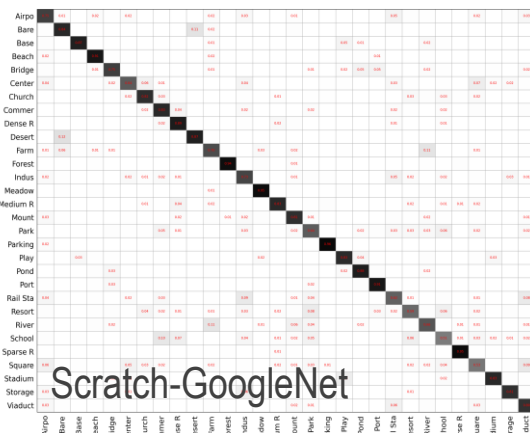
Results on AID

■ Accuracy comparison

Classification accuracy (%) on AID dataset using different initialization schemes

Metric	Pretrain dataset	AlexNet	VGG16	GoogleNet	ResNet101	DenseNet121	DenseNet169
OA	W/O	33.47 ± 2.15	72.18 ± 0.49	79.05 ± 0.89	49.46 ± 2.07	58.02 ± 0.74	59.16 ± 0.52
	ImageNet	88.79 ± 0.40	93.72 ± 0.21	92.24 ± 0.21	94.52 ± 0.25	94.68 ± 0.19	94.76 ± 0.21
	Million-AID	90.70 ± 0.43	95.33 ± 0.28	94.55 ± 0.23	95.40 ± 0.19	95.22 ± 0.26	95.24 ± 0.35
AA	W/O	33.85 ± 2.35	72.16 ± 0.54	78.88 ± 0.88	49.29 ± 2.06	57.88 ± 0.73	59.04 ± 0.51
	ImageNet	88.52 ± 0.39	93.38 ± 0.22	91.78 ± 0.23	94.18 ± 0.29	94.39 ± 0.21	94.44 ± 0.22
	Million-AID	90.46 ± 0.45	95.14 ± 0.27	94.30 ± 0.23	95.17 ± 0.19	94.97 ± 0.26	95.00 ± 0.38
Kappa	W/O	31.09 ± 2.24	71.19 ± 0.51	78.31 ± 0.92	47.63 ± 2.15	56.50 ± 0.76	57.69 ± 0.53
	ImageNet	88.39 ± 0.42	93.49 ± 0.21	91.96 ± 0.22	94.32 ± 0.26	94.49 ± 0.20	94.57 ± 0.22
	Million-AID	90.37 ± 0.44	95.17 ± 0.29	94.35 ± 0.24	95.24 ± 0.20	95.05 ± 0.27	95.07 ± 0.37

■ Confusion matrices of different learning schemes



Results on AID

■ Example images and predictions



The black labels are the ground truth. The orange labels indicate predictions by GoogleNet trained from scratch, the plum labels the predictions by DenseNet169 pre-trained on ImageNet, and the green labels the predictions by ResNet101 pre-trained on Million-AID.

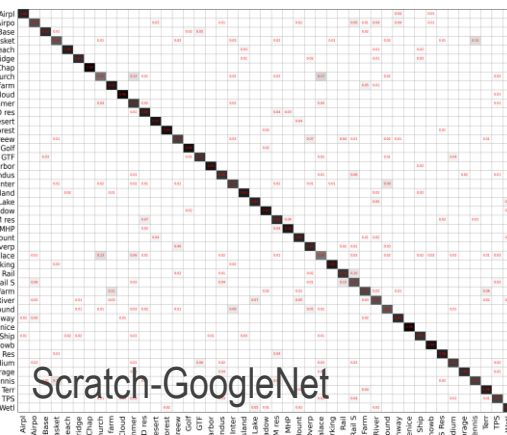
Results on NWPU-RESISC45

■ Accuracy comparison

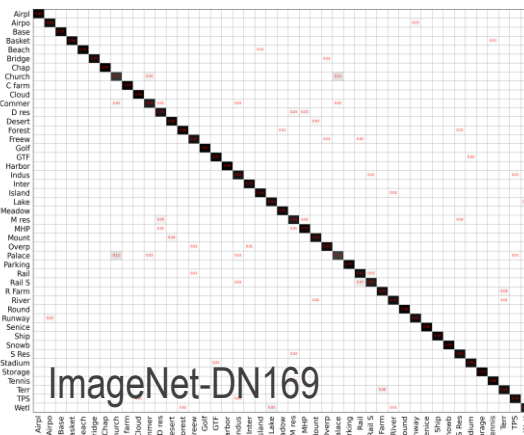
Classification accuracy (%) on NWPU-RESISC45 dataset using different initialization schemes

Metric	Pretrain dataset	AlexNet	VGG16	GoogleNet	ResNet101	DenseNet121	DenseNet169
OA	W/O	37.92 ± 0.70	73.19 ± 0.44	81.77 ± 0.56	58.82 ± 0.74	63.35 ± 0.34	64.51 ± 0.47
	ImageNet	87.19 ± 0.26	92.76 ± 0.18	91.71 ± 0.25	94.06 ± 0.16	93.90 ± 0.19	94.11 ± 0.20
	Million-AID	88.24 ± 0.21	93.62 ± 0.20	93.40 ± 0.23	94.20 ± 0.16	94.21 ± 0.20	94.26 ± 0.21
AA	W/O	37.92 ± 0.70	73.19 ± 0.44	81.77 ± 0.56	58.82 ± 0.74	63.35 ± 0.34	64.51 ± 0.47
	ImageNet	87.19 ± 0.26	92.76 ± 0.18	91.71 ± 0.25	94.06 ± 0.16	93.90 ± 0.19	94.11 ± 0.20
	Million-AID	88.24 ± 0.21	93.62 ± 0.20	93.40 ± 0.23	94.20 ± 0.16	94.21 ± 0.20	94.26 ± 0.21
Kappa	W/O	36.51 ± 0.72	72.59 ± 0.45	81.36 ± 0.58	57.89 ± 0.75	62.51 ± 0.35	63.70 ± 0.48
	ImageNet	86.89 ± 0.21	92.60 ± 0.19	91.52 ± 0.26	93.92 ± 0.17	93.76 ± 0.19	93.98 ± 0.20
	Million-AID	87.97 ± 0.21	93.48 ± 0.20	93.25 ± 0.24	94.07 ± 0.16	94.08 ± 0.20	94.13 ± 0.21

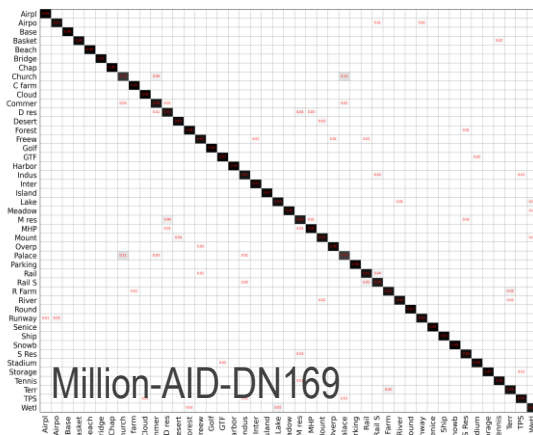
■ Confusion matrices of different learning schemes



Scratch-GoogleNet



ImageNet-DN169



Million-AID-DN169

Results on NWPU-RESISC45

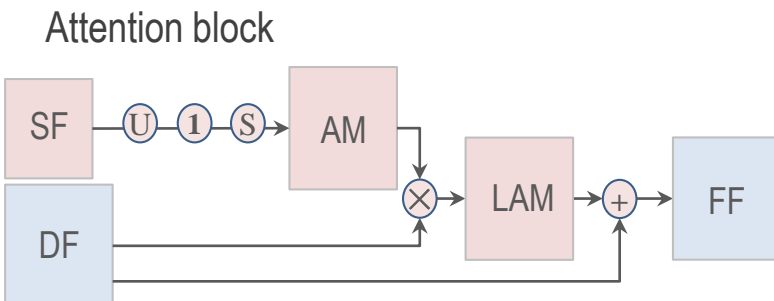
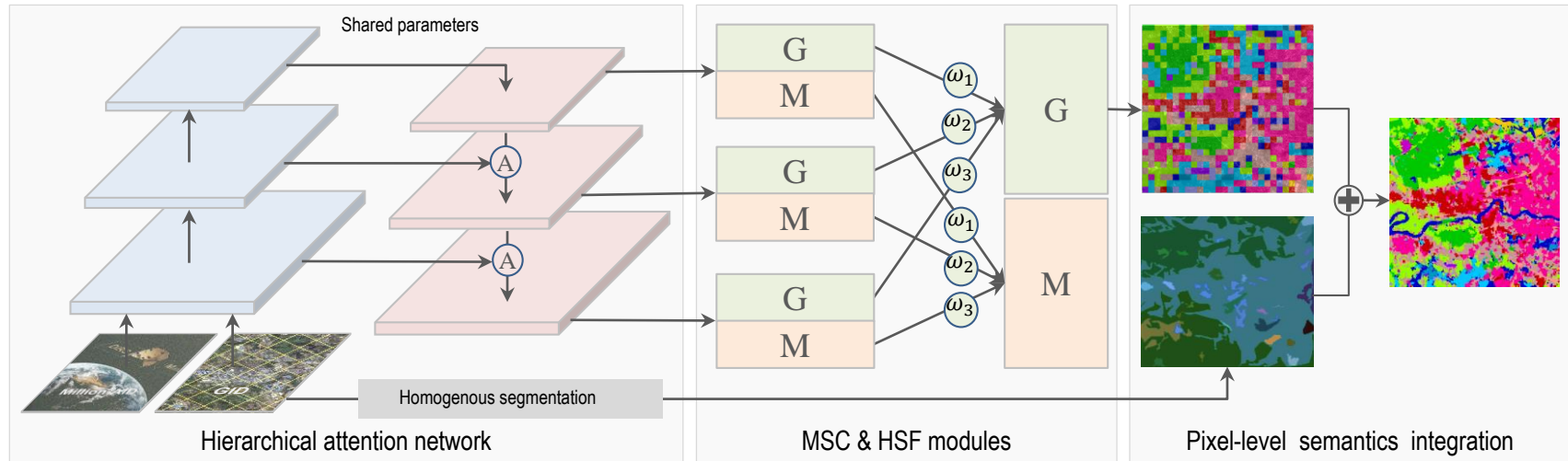
■ Example images and predictions



The black labels are the ground truth. The orange labels indicate predictions by GoogleNet trained from scratch, the plum labels the predictions by DenseNet169 pre-trained on ImageNet, and the green labels the predictions by ResNet101 pre-trained on Million-AID.

Semantic Classification

■ Transfer Knowledge from Million-AID for pixel-level image classification



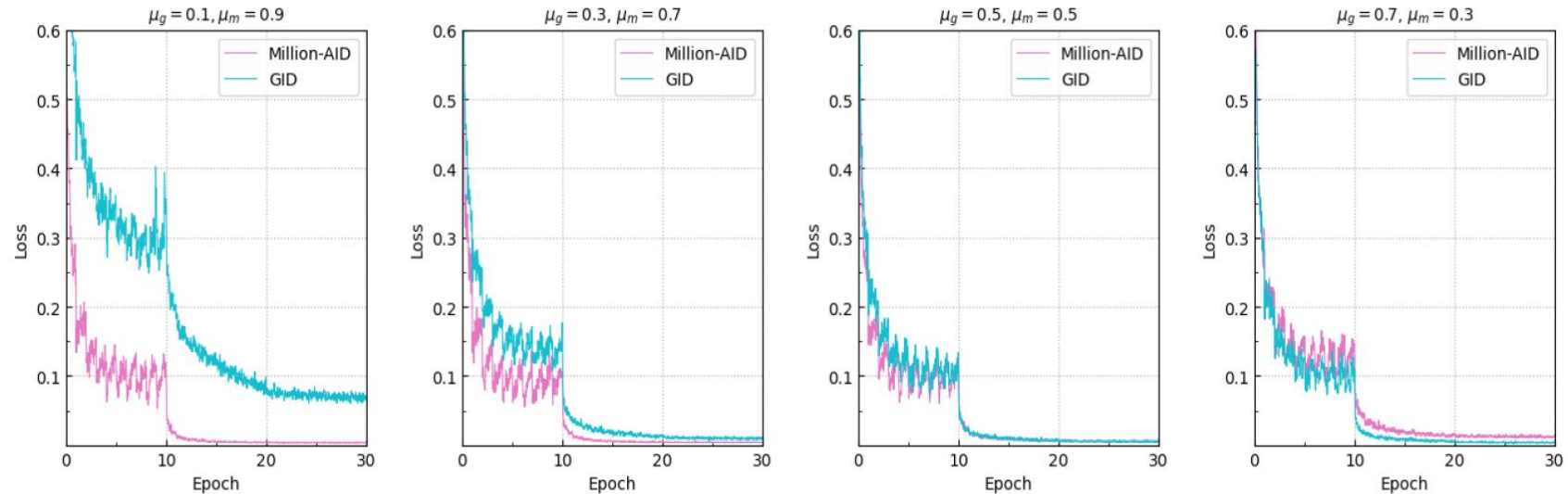
$$\begin{aligned}
 Loss^g &= \sum_{s=1}^S w_s CE_s^g \\
 \hat{p}_n(I) &= \frac{\sum_{s=1}^S w_s p_{s,n}(I)}{\sum_{s=1}^S w_s} \\
 Loss^m &= \sum_{s=1}^S w_s CE_s^m \\
 Loss &= \mu_g Loss^g + \mu_m Loss^m
 \end{aligned}$$

Ablation Study

- Weights influence of different tasks

μ_g	μ_m	GID			Million-AID		
		Kappa (%)	OA (%)	mIoU (%)	Kappa (%)	OA (%)	AA (%)
0.1	0.9	62.85	69.06	39.88	90.36	90.62	89.55
0.3	0.7	65.15	71.00	41.85	89.44	89.72	88.91
0.5	0.5	66.65	72.38	42.71	89.67	89.94	89.14
0.7	0.3	66.14	72.02	41.75	88.98	89.27	87.84

- Corresponding training loss observation



Comparison

Quantitative comparison using different Modules

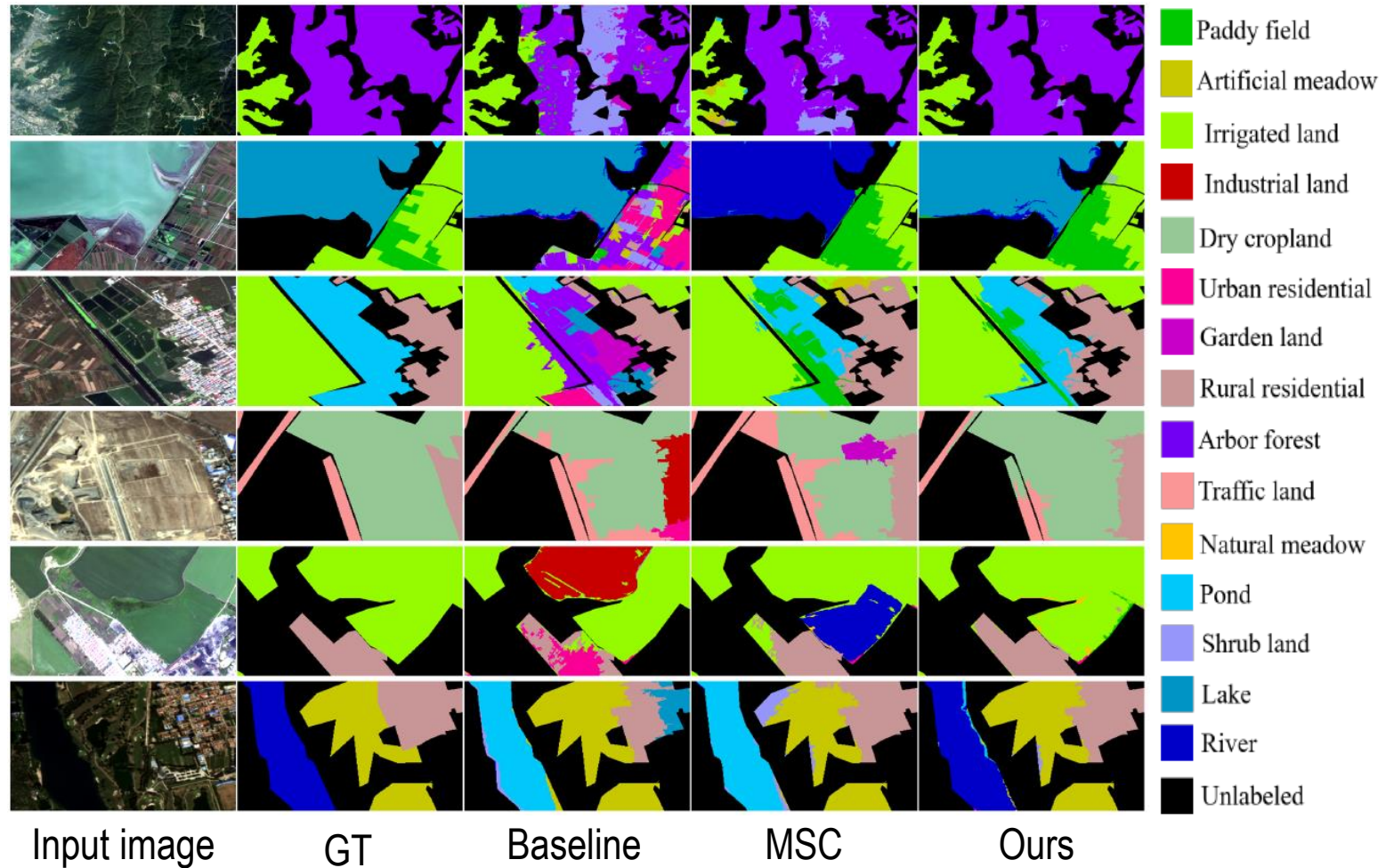
Baseline	MSC	HSR	HSI	Kappa (%)	OA (%)	mIoU (%)
✓				51.59	59.09	30.79
✓	✓			66.65	72.38	42.71
✓	✓	✓		66.79	72.52	43.07
✓	✓	✓	✓	67.33	73.03	43.68

Quantitative comparison with SOTA methods

Methods	Kappa	OA (%)
MLC + SGDL [141]	0.145	23.61
SVM + SGDL [141]	0.148	23.92
MLP + SGDL [141]	0.199	30.57
RF + SGDL [141]	0.237	33.70
DeepLab V3+ Mobilenet [199]	0.357	54.64
U-Net [197], [199]	0.439	56.59
PSPNet [198], [199]	0.458	60.73
DeepLab V3+ [199]	0.478	62.19
DeepLab V3+ MLF [199]	0.598	69.16
PT-GID [141]	0.605	70.04
Ours	0.673	73.03

Comparison

■ Qualitative comparison with different Modules



Input image

GT

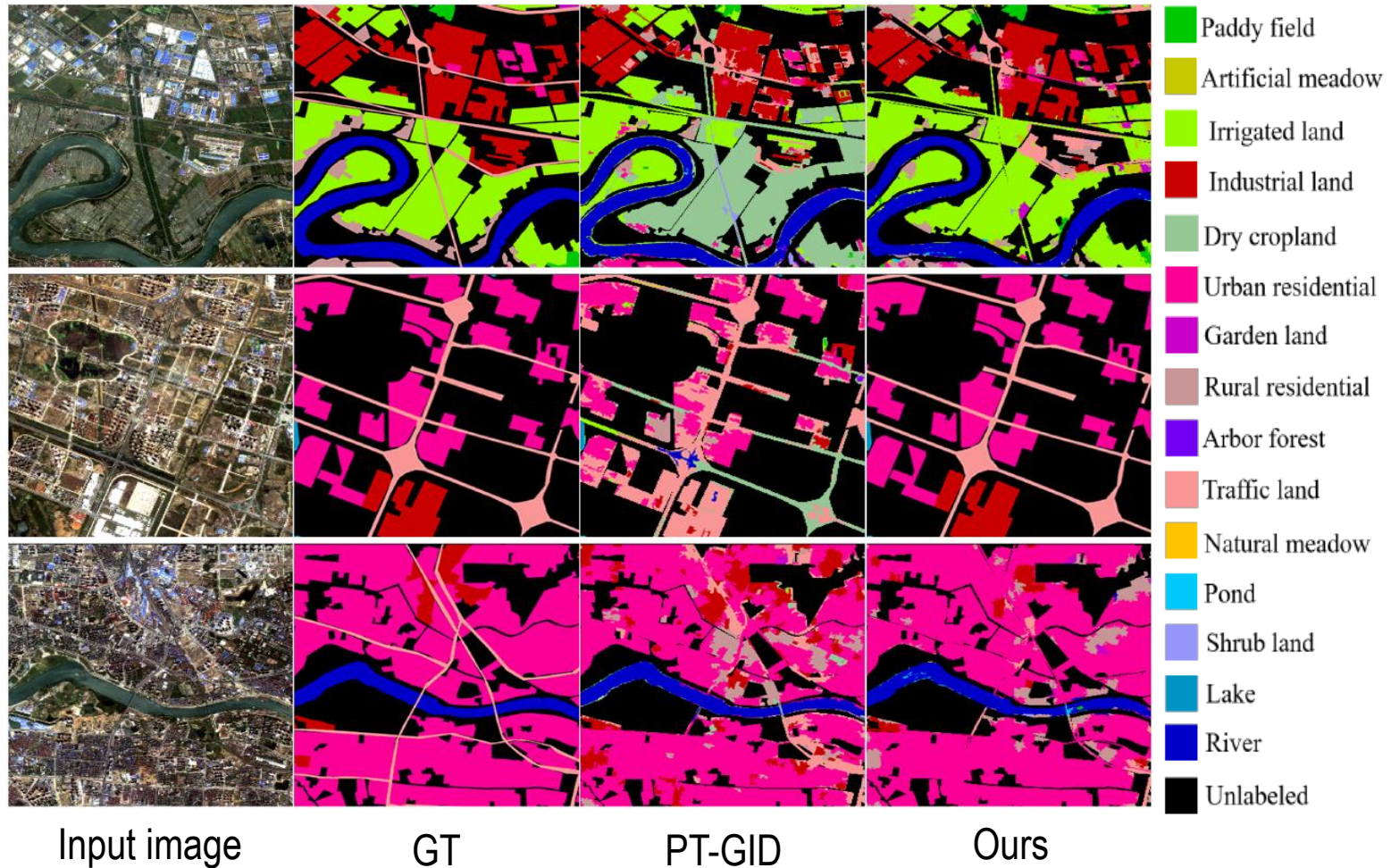
Baseline

MSC

Ours

Comparison

- Qualitative comparison with SOTA methods



Outline



- Background
- Revisiting Aerial Scene Recognition
- Introduction to Million-AID
- Aerial Scene Classification: A New Benchmark
- Knowledge Transfer: From Tile-level to Pixel-level
- Conclusions

■ A review of aerial image classification

- Classification prototypes develop with the improvement of image quality
- Per-pixel, object-based, and tile-level classification methodologies are established, relying on visual characteristics of images with different resolutions

■ Tile-level scene classification

- We released a large-scale and standard benchmark, for scene classification
- Million-AID shows better transferability than ImageNet for aerial scene classification

■ Pixel-level image parsing

- We verify the tremendous potential of transferring scene knowledge of Million-AID to advance aerial image interpretation from tile-level classification to pixel-wise parsing



CAPTAIN
COMPUTATIONAL AND PHOTGRAMMETRIC VISION

THANKS



*School of Computer Science, Wuhan University
Institute of Artificial Intelligence, Wuhan University
State Key Lab. LIESMARS, Wuhan University*

Gui-Song Xia (gusong.xia@whu.edu.cn)